Bulletin OEPP/EPPO Bulletin (2017) **47** (3), 384–400 ISSN 0250-8052. DOI: 10.1111/epp.12432

European and Mediterranean Plant Protection Organization
Organisation Européenne et Méditerranéenne pour la Protection des Plantes PM 7/39 (2)

Diagnostics
Diagnostic

PM 7/39 (2) *Aphelenchoides besseyi*

Specific scope

This Standard describes a diagnostic protocol for *Aphelenchoides besseyi.*

This Standard should be used in conjunction with PM 7/76 *Use of EPPO diagnostic protocols*.

Terms used are those in the EPPO Pictorial Glossary of Morphological Terms in Nematology[1].

Specific approval and amendment

Approved in 2003-09. Revised in 2017-04. This revision was prepared on the basis of the IPPC Diagnostic Protocol adopted in 2016 on *Aphelenchoides besseyi*, *Aphelenchoides fragariae* and *Aphelenchoides ritzemabosi* (Annex 17 to ISPM 27; IPPC, 2016). The EPPO Diagnostic Protocol only covers *A. besseyi.* It differs in terms of format but it is consistent with the content of the IPPC Standard for morphological identification for this species. With regard to molecular methods, one real-time PCR test available in the region is included as well as DNA barcoding.

1. Introduction

The most important host of *Aphelenchoides besseyi* is *Oryza sativa* (rice) and the consequent symptoms of damage have given rise to its common name, white-tip nematode of rice (Franklin & Siddiqi, 1972). *Aphelenchoides besseyi* also infests *Fragaria* species (strawberries), where it is the causal agent of 'summer dwarf' or 'crimp' disease. This nematode was recently identified as the causal agent of 'black spot disease' on beans (*Phaseolus vulgaris* L., Fabaceae) (Chaves *et al.*, 2013). In rice and strawberries, the nematode feeds ectoparasitically, but *A. besseyi* may also be endoparasitic. Specimens have been detected in soil of imported penjing (bonsai), but this may have happened due to the practice in China of irrigating the plants with water from paddy fields where the nematode is present. The nematode is capable of withstanding desiccation, and may be found in a quiescent state beneath the hulls of rice grains.

A flow diagram describing the diagnostic procedure for *A. besseyi* is presented in Fig. 1.

[1]http://www.eppo.int/QUARANTINE/diag_activities/EPPO_TD_1056_Glossary.pdf.

2. Identity

Name: *Aphelenchoides besseyi* Christie 1942
Synonyms: *Aphelenchoides oryzae* Yokoo 1948
Asteroaphelenchoides besseyi (Christie 1942) Drozdovsky 1967
Taxonomic position: Nematoda: Aphelenchida: Aphelenchina: Aphelenchoididae: *Aphelenchoides*
EPPO Code: APLOBE
Phytosanitary categorization: EPPO A2 List no. 122; EU Annex designation: II/A1 on rice and II/A2 on strawberry.

3. Detection

3.1. Symptoms

3.1.1. Oryza sativa

During early growth of *O. sativa*, the most conspicuous symptom caused by this nematode is the emergence of the chlorotic tips of new leaves from the leaf sheath (Figs 2 and 3). These tips later dry and curl, while the rest of the leaf may appear normal. The young leaves of infested tillers can be speckled with a white splash pattern or have distinct chlorotic areas. Leaf margins may be distorted and wrinkled, but leaf sheaths are symptomless. The flag leaf enclosing the panicle crinkles and distorts, and the panicle

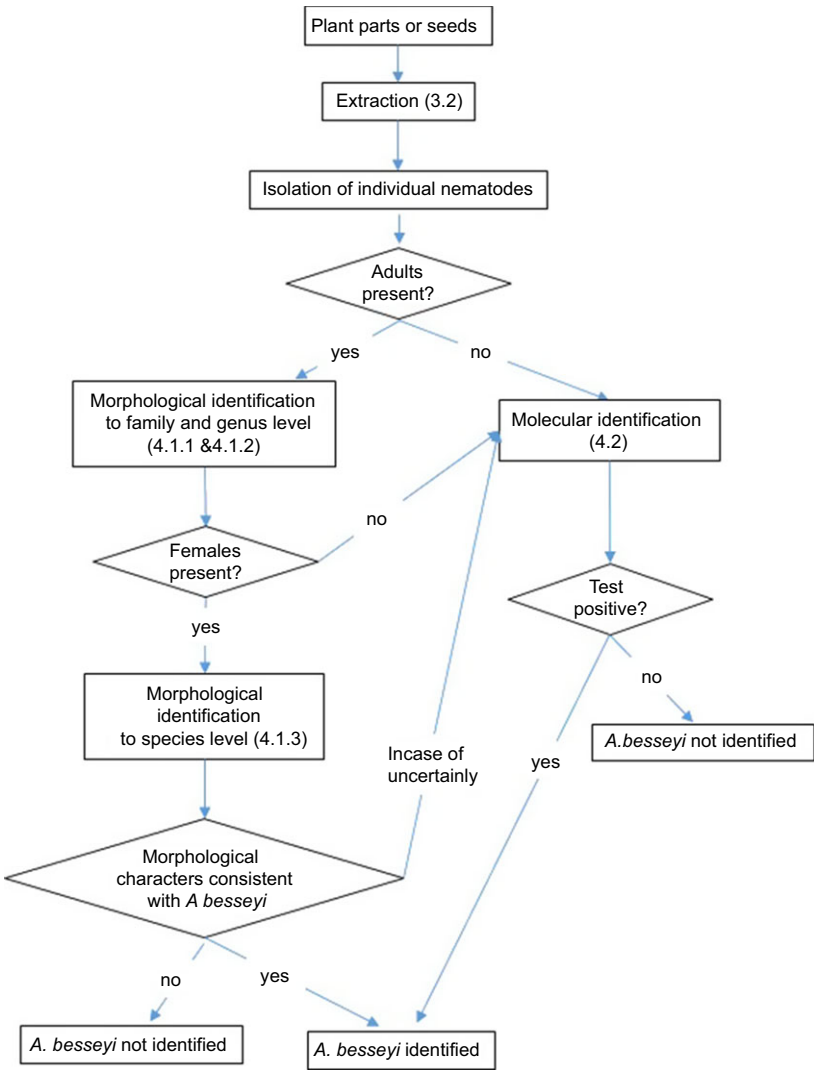

Fig. 1 Flow diagram for the detection and identification of *Aphelenchoides besseyi*. [Colour figure can be viewed at wileyonlinelibrary.com]

is reduced in size, as are the grains. Symptoms may be confused with those of calcium and magnesium deficiency. Infested panicles are shorter than normal panicles, with fewer spikelets and a smaller proportion of filled grain (Dastur, 1936; Yoshii and Yamamoto, 1951; Todd and Atkins, 1958). In severe infestations, the shortened flag leaf is twisted and can prevent the complete extrusion of the panicle from the boot (Yoshii and Yamamoto, 1950; Todd and Atkins, 1958). The panicles also often stay erect (Liu *et al.*, 2008) and discoloration can be observed on them (CABI, 2013). The grain is small and distorted (Todd and Atkins, 1958) and the kernel may be discolored and cracked (Uebayashi *et al.*, 1976) (Fig. 3). Infested plants mature late and have sterile panicles borne on tillers produced from high nodes.

3.1.2. Fragaria spp.

On *Fragaria* species, *A. besseyi* is the causal agent of 'summer dwarf disease' (Perry and Moens, 2006) (Fig. 4). Symptoms include leaf crinkling and distortion, and dwarfing of the plant with an associated reduction in flowering (Fig. 4). Symptoms may be similar to, and therefore confused with, those caused by other *Aphelenchoides* species, emphasizing the importance of correct identification.

3.1.3. Other hosts

In *Ficus elastica* and *Polianthes tuberosa* the nematode is endoparasitic, and causes leaf drop and leaf lesions, respectively. On *Capsicum annum* var. *longum* the infestation appears to result in rotting of the pods and premature pod drop, similar to some fungal diseases (Hockland and Eng, 1997). In the grass *Sporobolus poirettii*, this nematode stimulates growth, resulting in increased flowering. The nematode has also been found on *Boehmeria nivea*, numerous ornamental plants (including chrysanthemum, *Hibiscus* and *Saintpaulia ionantha*) and grasses (*Panicum*, *Pennisetum* and *Setaria*).

Fig. 2 Symptoms on rice. (Courtesy Adnan Tülek, Directorate of Trakya Agricultural Research Institute, Turkey.)

Fig. 3 Infested (right) and non-infested (left) grains of rice. Courtesy Adnan Tülek, Directorate of Trakya Agricultural Research Institute, Turkey.

3.2. Extraction from plant material

3.2.1. Direct examination

In leaves infested with *A. besseyi,* nematodes can be detected by inspecting cut leaves, especially small and young ones, immersed in tap water in a Petri dish under a stereomicroscope (the nematodes will swim into the water within 30 min if there is a heavy infestation).

3.2.2. Extraction methods

Extraction methods from different substrates (seeds, plant material and soil) are described in EPPO Standard PM 7/119 on nematode extraction (EPPO, 2013).

For seeds, the methods recommend the use of whole seeds, but Moretti *et al.* (1999) recommends the use of rice chaff or hull as an alternative testing material. A highly efficient method using dehulled seeds has been published by the International Seed Testing Association (ISTA, 2017) and is described in Appendix 1. The minimum sample size recommended by the ISTA is 1000 seeds. In any case, the maximum subsample size should be 250 seeds.

Fig. 4 Symptoms caused by *Aphelenchoides besseyi* on strawberry. Photo courtesy Jeffrey Lotz, Florida Department of Agriculture and Consumer Services, Gainesville, FL, United States.

For plant material the Baermann funnel/Oostenbrink dish methods should be run for at least 48 h in order to detect low levels of infestation.

3.3. Microscope examination of extracts and preparation of slides

All developmental stages (females, males and juveniles) can be extracted from infested plant tissues or soil. Under

the stereomicroscope, the round, relatively large median bulb is a distinctive feature of nematodes belonging to the order Aphelenchida. These nematodes are vermiform, with most species appearing to be of stout structure and slow-moving. However, species such as *A. besseyi* and leaf and bud nematodes tend to be of slim build, pale appearance, relatively long when compared to most other *Aphelenchoides* spp. and good 'swimmers' (with a serpentine motion) in water (however, *Aphelenchoides blastophthorus*, a pest of ornamental plants and strawberries, rarely 'swims' well and is of stouter structure).

Aphelenchoides spp. can be picked from extracts and a temporary mount made on a glass slide. Nematodes are collected into a drop of water on a slide, which is then slowly heated (to approximately 60°C) until the nematodes become immobile. The body of *A. besseyi* killed by gentle heat is almost straight. The nematodes can be sealed on the slide with wax during this process or they can be placed in a drop of fixative before sealing with wax. There is some difference in the appearance of specimens in water and fixed specimens (for diagnostics the former is being preferable) but in fixed preparations some features such as stylets become more distinct. The examination then continues using a high power microscope (with at least ×1000 magnification for examination under oil immersion).

3.4. Molecular tests

Molecular tests can be performed on floats (see section 4).

4. Identification

Although *A. besseyi* can be identified to species level based on morphological examination, this is possible only for adult specimens, as is the case for most other plant-parasitic nematode species. For precise species-level identification, the morphological characters of *Aphelenchoides* species need to be carefully examined under a high-power microscope with at least ×1000 magnification for use with immersion oil. It is recommended that this is done in combination with differential interference contrast microscopy. If available, scanning electron microscopy is helpful in determination of lateral field and tail characteristics.

Because *Aphelenchoides* species are very difficult to identify to species level using morphological characters alone, molecular diagnostic tools have been developed to support their morphological identification (Ibrahim *et al.*, 1994a,b). Molecular methods can be applied to identify all life stages, including the immature stages, and may be particularly helpful when there is a low level of infestation or when adult specimens are atypical or damaged. However, the specificity of currently available molecular tests may be limited as they have generally been developed and evaluated using a restricted number of species and populations from different geographical regions.

4.1. Morphological identification

4.1.1. Identification of the family Aphelenchoididae

The family Aphelenchoididae is characterized by a large metacorpus and pharyngeal glands not usually enclosed in a bulb (overlapping). The dorsal pharyngeal gland opens into the metacorpus. Males have caudal papillae. The main morphological characteristics shared by the family Aphelenchoididae are presented in Table 1.

Table 1. Main morphological characteristics shared by the family Aphelenchoididae

Body part	Characteristic
Body form	Vermiform, not swollen
Lateral field	With four or fewer incisures (two to four, rarely six)
Stylet	Slender, with narrow lumen and usually with small basal knobs or swellings
Pharynx	Isthmus rudimentary or absent, nerve ring circumintestinal or circumpharyngeal, pharyngeal glands lobe-like and long dorsally overlapping intestine
Post-uterine sac	Usually present
Spicule	Rose thorn-shaped or derived therefrom
Adanal bursa	Rarely present (reported to date only from *Pseudaphelenchus*)
Gubernaculum	Absent
Tail shape	Both sexes similar, conoid, with pointed or rounded, often mucronate (one or more mucros) terminus

4.1.2. Identification of the genus Aphelenchoides

As with many other nematode genera, *Aphelenchoides* species are morphologically very similar; these nematodes are vermiform, with most species appearing stout and slow-moving. However, the few economically important species such as *A. besseyi*, *A. fragariae* and *Aphelenchoides ritzemabosi* tend to be slim, pale and relatively long when compared with most other *Aphelenchoides* species.

The morphological characteristics of the genus are as follows:

- body length from 0.2 to 1.3 mm, but most commonly from 0.4 to 0.8 mm
- heat-relaxed females become straight to ventrally arcuate (Fig. 5A)
- heat-relaxed males assume a walking-stick shape with the tail region curled ventrally (Fig. 5B)
- cuticle finely annulated, lateral field with two to four (rarely six) incisures (Fig. 5D)
- stylet very difficult to see under low-power microscopy; under high power, the stylet varies from clearly discernible to very faint and generally, about 10–12 µm long; similarly, basal knobs or swellings are sometimes clear but often indistinct
- pharynx: pharyngeal procorpus long and slender; metacorpus well developed, spherical to rounded-rectangular,

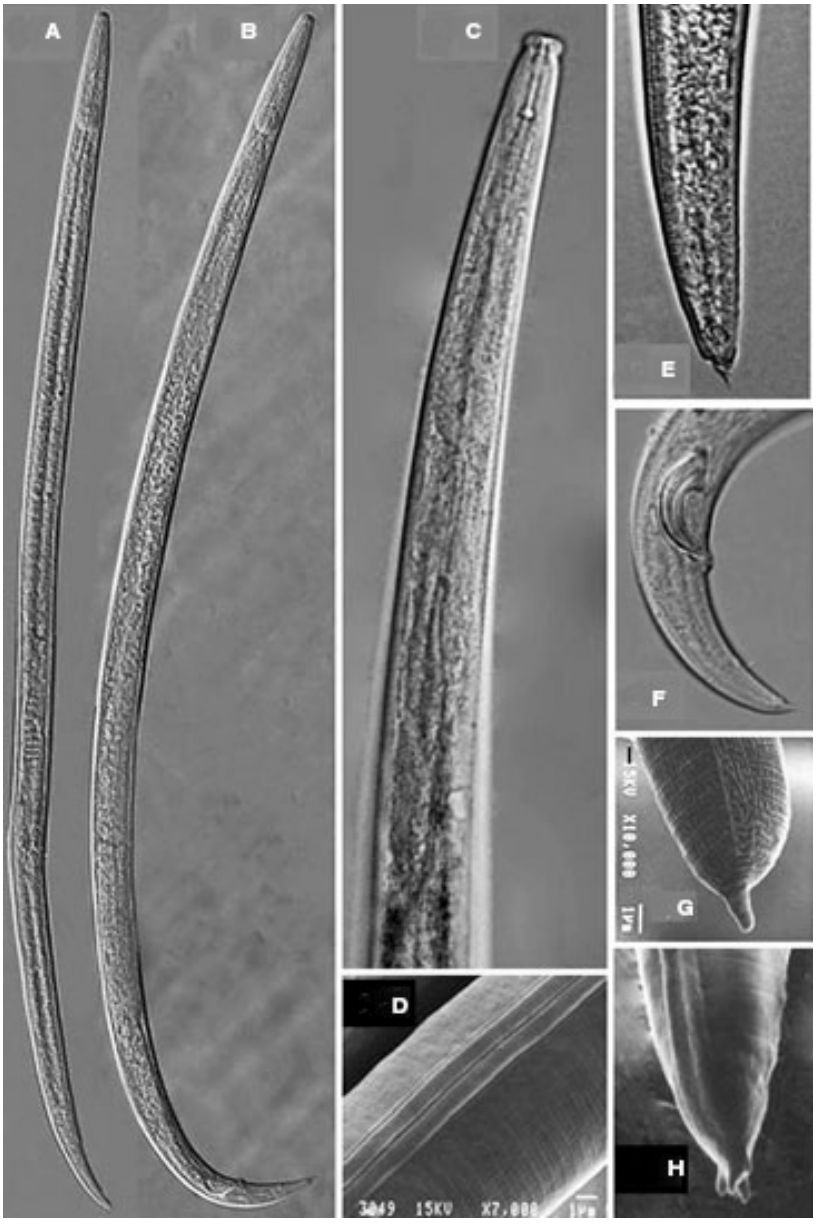

Fig. 5 *Aphelenchoides* species: (A) female; (B) male; (C) female anterior end; (D) lateral field; (E) female tail; (F) male tail; (G) female tail terminal mucro; and (H) male tail terminal mucro.
Source: (A, B, E) Wang *et al.* (2013); (D, G) Deimi *et al.* (2006); (H) Yu and Tsay (2003); (C, F) photos courtesy Z. F. Yang and H. Xie, South China Agricultural University, Guangzhou, China).

with central metacorpus plates; pharyngeal gland lobe long, with dorsal overlap of the intestine (Fig. 5C)
- vulva typically post-median, usually between 60 and 75 per cent of the body length
- ovary monoprodelphic, typically outstretched, but may be flexed
- post-vulval sac almost always present
- tail shape conoid to variable (Fig. 5E, F), in males more strongly curved ventrally and papillae variable
- tail terminus without or with one or more mucros (Fig. 5G, H) (a mucro is defined as a structure at the end of the tail terminus). Mucros can be definitively discerned only at ×1000 with oil immersion. The presence or absence of mucros, and the shapes they assume, can be used to distinguish species, and are a key element in the identification of *A. besseyi*
- spicules well-developed, thorn-shaped, paired and separate
- bursa absent.

Aphelenchoides spp. can be distinguished from species of other genera encountered in soil and plant material by using the key in Table 2.

4.1.3. Identification of A. besseyi

The identification of species in the *Aphelenchoides* genus is complex and requires a systematic approach. It is generally agreed that a combination of morphological and molecular methods is required for the most reliable identification. The

Table 2. Key to distinguish adult individuals of *Aphelenchoides* species from species of other genera in soil and plant material

1	Stylet present	2
	Stylet absent	NAS
2	Four-part pharynx with cylindrical procorpus, metacarpus with plates, slender isthmus and glandular basal bulb	3
	Two-part pharynx, anterior part slender, posterior part expanded, glandular and muscular	NAS
3	Dorsal pharyngeal gland outlet in metacorpus; metacorpus very large, often appears nearly as wide as the diameter of the body	4
	Dorsal pharyngeal gland outlet in procorpus behind stylet knobs; metacorpus moderate to reduced in size (less than three-fourths body width)	NAS
4	Pharyngeal glands lobe-like, long dorsal overlap of intestine	5
	Pharyngeal glands pyriform, not overlapping intestine; or pharyngeal glands lobe-like, ventral overlap of intestine	NAS
5	Lateral fields with four or fewer incisures*; stylet with basal knobs or swellings; female tail conoid, elongate conoid, convex conoid or subcylindrical to a pointed or narrowly rounded terminus; male spicules robust, thorn-shaped; adanal bursa absent	6
	Lateral fields with six or more incisures; stylet without basal knobs; female tail short, subcylindroid and with broadly rounded terminus; male spicules slender, tylenchoid; adanal bursa present	NAS
6	Tails of both sexes short, usually less than four times anal body width	7
	Tails of both sexes elongate to filiform, usually more than four times anal body width	NAS
7	Stylet slender, often about 10–12 μm and usually less than 20 μm; vulval flap absent; male without small bursa-like flap at tail tip	*Aphelenchoides*
	Not with the above combination of characters	NAS

NAS, not *Aphelenchoides* species.

*Khan *et al.* (2012) reports populations having lateral fields with 6 incisures (additional information compared to the IPPC Diagnostic Protocol; IPPC, 2016).

first step in diagnosis is to record and measure the critical morphological features of as many female specimens as are available, ideally 20. In practice, far fewer adult specimens are usually available, and in such cases the nematologist should prepare the specimen(s) with great care to avoid damaging the few features available, leaving sufficient juveniles or females for analysis by molecular tools. Males are not included in the keys presented in this diagnostic protocol, but the shape and size of their spicules may assist in confirming the final identification.

Sanwal (1961) produced a dichotomous key to 35 *Aphelenchoides* species that were recognized at the time, but to date over 180 species have been described (Sánchez-Monge *et al.*, 2015). Allen (1952) provided a key to the four species of bud and leaf nematodes (*A. besseyi*, *A. fragariae*, *A. ritzemabosi* and *Aphelenchoides subtenuis*). Sanwal (1961) produced a dichotomous key to the 35 *Aphelenchoides* species that were recognized at the time. Fortuner (1970) devised a dichotomous key to 11 *Aphelenchoides* species with star-shaped mucros. Baranovskaya (1981) provided a dichotomous key to 97 species with descriptions of 105 species. Shahina (1996) provided a compendium to 141 *Aphelenchoides* species. EPPO (2004) devised a polytomous key to 17 *Aphelenchoides* species including 14 species with star-shaped mucros and 3 species of bud and leaf nematodes without star-shaped mucros (*A. blastophthorus*, *A. fragariae* and *A. ritzemabosi*). This key is updated in this revised protocol.

It should be noted that *Aphelenchoides* species other than *A. besseyi* can occur in soil, foliage and rice husks. Many of these nematodes are difficult to identify because few characters allow their distinction and most species are poorly described (Sánchez-Monge *et al.*, 2015). Indeed, several authors have improved the original description for *A. besseyi*. In addition, studies on this species have shown the degree of variation in measurements made on populations from different hosts.

Hockland (2002) has therefore attempted to reduce the number of comparisons that need to be made by selecting only those *Aphelenchoides* species that also have a star-shaped mucro, together with those pest species that might also be encountered in foliage. This following procedure relies heavily on the original descriptions and drawings of species, which at times can appear contradictory. For example, the tail shape for *Aphelenchoides aligarhiensis* is described as elongate-conoid, but the accompanying drawing does not infer this. There is also no accompanying value for '*c*', which is an indicator of tail shape, being the value of tail length divided by body width at the anus. Similarly, the excretory pore for *Aphelenchoides jonesi* is said to be opposite the nerve ring, but the accompanying drawing infers that it is posterior to the nerve ring. In such cases the written description has been the one included in this Protocol. Where possible, original data has been supplemented by additional published information for the most commonly encountered species.

4.1.3.1. Description of Aphelenchoides besseyi

This description is modified from Hunt (1993). Figure 10 illustrates the main diagnostic features of the species.

Table 3. Dichotomous key to female *Aphelenchoides* species

1.	Star-shaped mucro	2
	No star-shaped mucro	Not *A. besseyi*
2.	Post-vulval sac length up to 33% of distance from vulva to anus	3
	Post-vulval sac length more than 33% of distance from vulva to anus	*A. aligarhiensis*, *A. brevistylus*, *A. fujianensis*, *A. lichenicola*
3.	Tail shape conoid or elongate conoid	4
	Tail shape subcylindrical	*A. siddiqii*
4.	Stylet length 10–12.5 µm	5
	Stylet length outside the range 10–12.5 µm	*A. asteromucronatus*, *A. hylurgi*, *A. wallacei*
5.	Four lateral lines	6
	Fewer or more than four lateral lines	*A. andrassyi*, *A. asterocaudatus*, *A. unisexus*
6.	Excretory pore anterior to, or level with, anterior level of nerve ring	*A. besseyi*
	Excretory pore level with nerve ring	*A. goodeyi*, *A. jonesi*, *A. silvester*

Female: Body slender, straight to slightly arcuate ventrally when relaxed. Cephalic region rounded, unstriated, slightly offset and wider than body at lip base. Lateral fields about one-fourth as wide as body, with four incisures. Metacorpus oval, with distinct metacorpus plates slightly behind its centre. Excretory pore usually near the anterior edge of the nerve ring. Post-vulval sac narrow, inconspicuous, not containing sperm, 2.5–3.5 times anal body width but less than one-third the distance from the vulva to the anus. Tail conoid, 3.5–5 anal body widths long. Terminus bearing a mucro of diverse shape with three to four pointed processes.

Male: Often as numerous as females. Posterior end of body curved by about 180 degrees in relaxed specimens. Tail conoid, with terminal mucro with two to four pointed processes. Spicules typical of the genus except that the proximal ends lack a distinct apex and have only a moderately developed rostrum. The dorsal limb spicules measure 18–21 µm (mean 19.2 µm).

4.1.3.2. Dichotomous key

A short dichotomous key prepared for this Protocol is presented Table 3. Only characters from female nematodes have been considered. This is complemented by Figs 6–9 showing critical features, and Fig. 10, giving more details of those *Aphelenchoides* species that also have a star-shaped mucro, together with those pest species that might also be encountered in foliage.

4.1.3.3. Polytomous key

Several key features have been selected to produce a small polytomous key (Table 4). The selected features have been given codes: the shape of the mucro (A), post-vulval sac length (B), tail shape (C), stylet length (D), the number of lateral lines (E) and the relative positions of the excretory pore and nerve ring (F).

Each specimen should therefore be examined and assigned a set of codes according to the following categorization.

A, mucro shape	1 = star (Fig. 7A–F); 2 = single terminal mucro (Fig. 7G–M); 3 = bifurcate (Fig. 7N); 4 = other (Fig. 7O–T); 5 = no mucro (Fig. 7U–V)
B, post-vulval sac length (pvs)	1 = pvs length 33% or less of the distance between the vulva and the anus; 2 = pvs length more than 33% of the distance between the vulva and the anus; 3 = no pvs
C, tail shape	1 = conoid: shape of a cone, with both sides of the tail surface tapering at an equal angle to the tail tip. Total length not exceeding 5 times anal body width (Fig. 8A); 2 = elongate-conoid: an elongated cone, with a length 5 or more anal body widths long (Fig. 8B,C); 3 = dorsally convex-conoid: tail shape that at its first appearance is curved ventrally. The dorsal side of the tail is curved in a convex manner before it joins with the ventral surface. The ventral surface is usually concave, but from some viewpoints may appear straight. It may be any length (Fig. 8D,E); 4 = subcylindroid: both sides of the tail appear to run parallel for most of their length, and end with a hemispherical or sub-hemispherical tail tip (Fig. 8F).
D, stylet length (µm)	1 = 10–13; 2 = less than 10; 3 = more than 13
E, lateral lines (number of)	1 = 4 lines; 2 = 3 lines; 3 = 2 lines; 4 = unknown
F, relative position of the excretory pore and nerve ring	1 = excretory pore anterior to, or level with, the anterior level of the nerve ring (Fig. 9A,B); 2 = excretory pore level with the nerve ring (Fig. 9C); 3 = excretory pore posterior to or opposite the posterior level of the nerve ring (Fig. 9D,E)

Compared to the IPPC protocol, supplementary drawings of the types of mucros and tail shapes are provided in Fig. 10 to aid categorization.

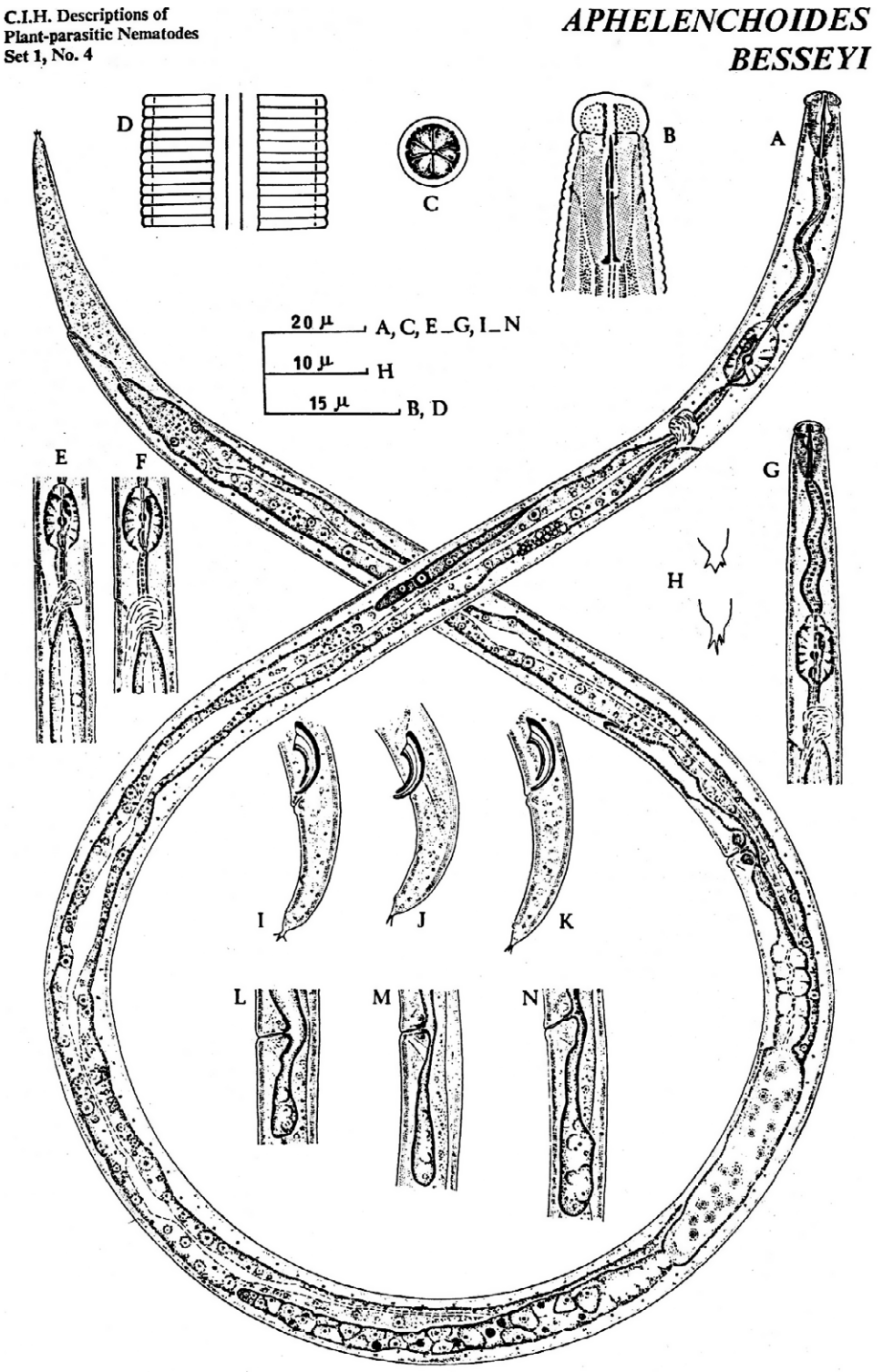

Aphelenchoides besseyi Christie. A. Female. B. Female head end. C. Female *en face* view. D. Lateral field. E & F. Variation in female median oesophageal bulb and position of excretory pore with respect to nerve ring. G. Male anterior end. H. Female tail termini showing variation in shape of mucro. I–K. Male tail ends. L–N. Variation in post-vulval uterine sac. (B and D original: the rest after Fortuner, 1970.)

Fig. 6 *Aphelenchoides besseyi*.

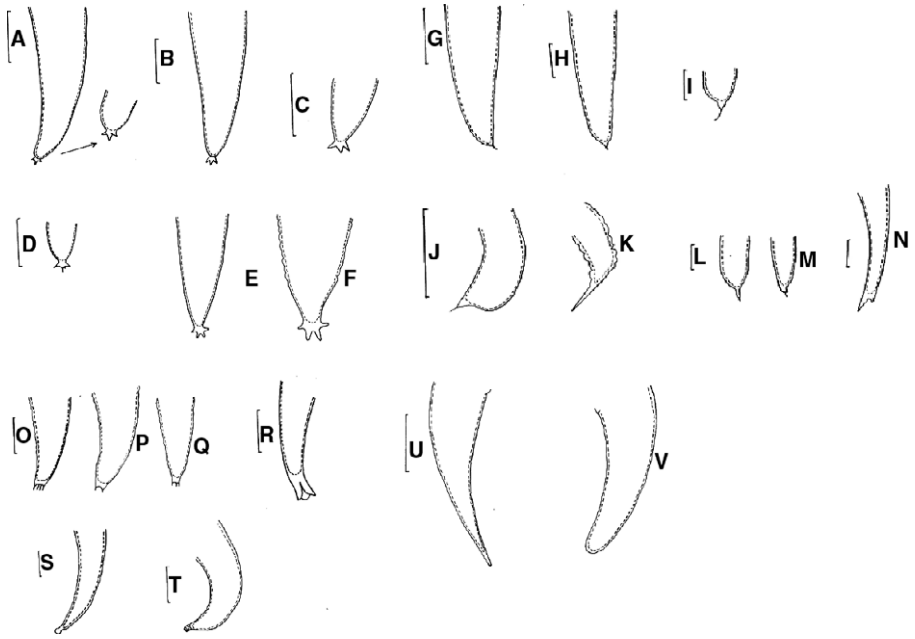

Fig. 7 Tail terminus types of *Aphelenchoides* species (after Hockland, 2002).
Star shape: (A) *A. aligarhiensis*, (B) *A. asterocaudatus*, (C) *A. besseyi*, (D) *A. goodeyi* (all scale bars 10 μm), (E) and (F) *A. nonveilleri* (×1100 and ×2200, respectively).
Single terminal mucro: (G) *A. richardsoni*, (H) *A. nechaleos*, (I) *A. vaughani*, (J) *Aphelenchoides* sp., (K) *A. tsalolikhini*, (L, M) *A. submersus*
Bifurcate, (N) *A. bicaudatus* (all scale bars 10 μm).
Other: (O, P, Q) *A. ritzemabosi*, (R) *A. sphaerocephalus*, (S) *A. gynotylurus*, (T) *A. helicosoma* (scale bars all 10 μm).
No mucro: (U) *A. microstylus* (scale bar 10 μm), (V) *A. obtusus* (×1250).

The set of codes obtained should then be compared with those set out in Table 4, which should allow a provisional diagnosis to be made.

As with all identifications involving the use of morphological characters, the combination of several key features is the key to a positive diagnosis. In the polytomous key there is some overlap of codes, and users are advised to refer to original descriptions if in doubt about a diagnosis, or refer to the database (see Appendix 4 for further guidance). Alternatively, a dichotomous key, using the same set of characters, may also help to determine the identity of the nematode.

4.1.4. Possible confusion with similar species

Aphelenchoides besseyi differs from other plant-parasitic species of the genus by having a star-shaped mucro, although non-pathogenic species of *Aphelenchoides* may also have star-shaped mucros. These species can be distinguished from *A. besseyi* by following the guidance given in the keys. Those species that remain indistinguishable apart from the position of the excretory pore, a feature that is often difficult to see, can be further distinguished by additional features: *Aphelenchoides goodeyi* has a convex-conoid tail and is generally shorter in its body length (0.46–0.61 mm compared with 0.57–0.88 mm for *A. besseyi*); *A. jonesi* generally has a lower value for '*a*' (20–28, compared

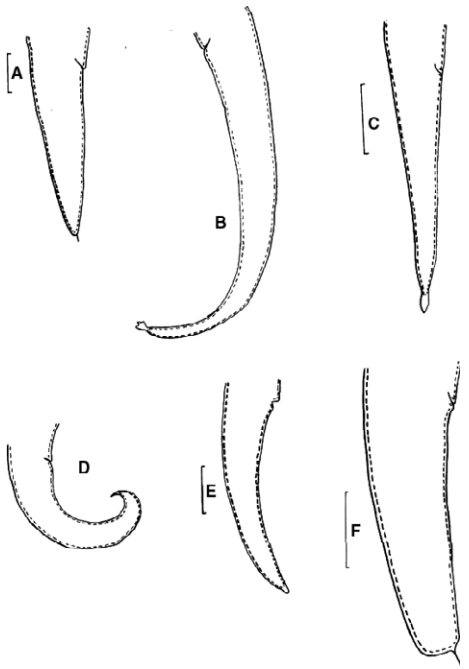

Fig. 8 Drawings of tail shapes in *Aphelenchoides* species. Conoid: (A) *A. blastophthorus.* Elongate-conoid: (B) *A. andrassyi* (no scale bar), (C) *A. chalonus.* Dorsally convex-conoid: (D) *A. fluviatilis* (×1100), (E) *A. franklini.* Sub-cylindroid: (F) *A. subtenuis*. Scale bars 10 μm.

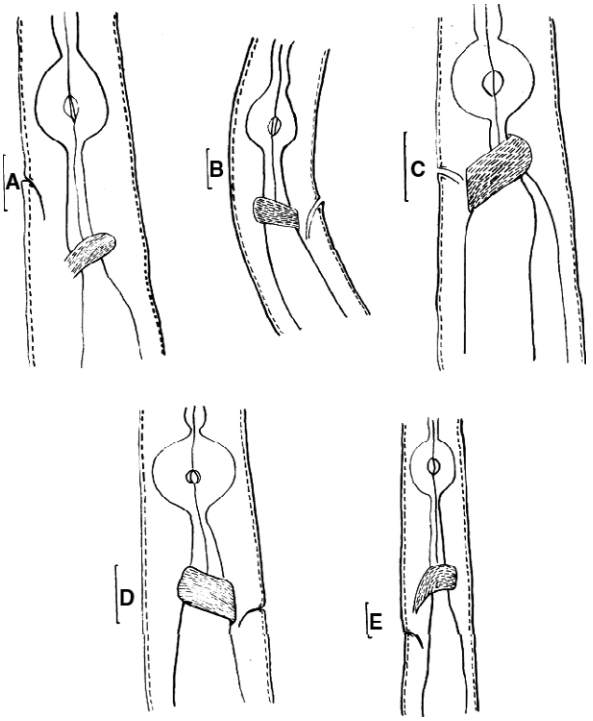

Fig. 9 Positions of the excretory pore relative to the nerve ring in *Aphelenchoides* species. Excretory pore is anterior to or level with the anterior edge of the nerve ring: (A) *A. longiurus*, (B) *A. blastophthorus.* Excretory pore is level with the nerve ring (from behind the anterior point to in front of the posterior point): (C) *A. cibolensis.* Excretory pore is level with the posterior edge of the nerve ring, (D) *A. arcticus*, or posterior to it, (E) *A. ritzemabosi*. Scale bar 10 μm.

with 26–58) and a slightly higher range of values for its stylet length (11–14 μm, compared with 10–12.5 μm); *Aphelenchoides silvester* has a convex-conoid tail shape, a slightly lower value for '*b*' (8–9.7, compared with 9–13.1) and is generally shorter in body length (0.48–0.56 mm, compared with 0.57–0.88 mm). Males are commonly found when *A. besseyi* is numerous, but they have not been described for *A. goodeyi*, *A. jonesi* or *A. silvester*.

Apart from the shape of the mucro, *A. besseyi* differs from other plant-parasitic species of this genus occurring in strawberries (*A. blastophthorus*, *A. fragariae* and *A. ritzemabosi*) as follows: *A. besseyi* has a post-vulval sac that is always less than a third of the distance from the vulva to the anus, whereas those of the other species are longer than this; the tail of *A. besseyi* has a conoid shape, similar to *A. blastophthorus*, but shorter than that of *A. fragariae* and *A. ritzemabosi*, which tend to be elongate-conoid; the excretory pore is usually positioned near the anterior edge of the nerve ring in *A. besseyi*, whereas in the other species it is either level with or posterior to the nerve ring; the spicules of *A. besseyi* are distinctive in that the proximal end lacks a dorsal process (or apex) and has only a moderately developed ventral one (rostrum), whereas those of *A. blastophthorus* are comparatively large for the genus, have a rather stout dorsal limb, which is characteristically flattened about mid-way along its arch, its distal end is curved ventrally to give it a hooked or knobbed appearance, and the apex and rostrum are pronounced structures; those of *A. fragariae* have a moderately developed apex and rostrum, whilst the smoothly curved spicules of *A. ritzemabosi* seem to lack a dorsal or ventral process.

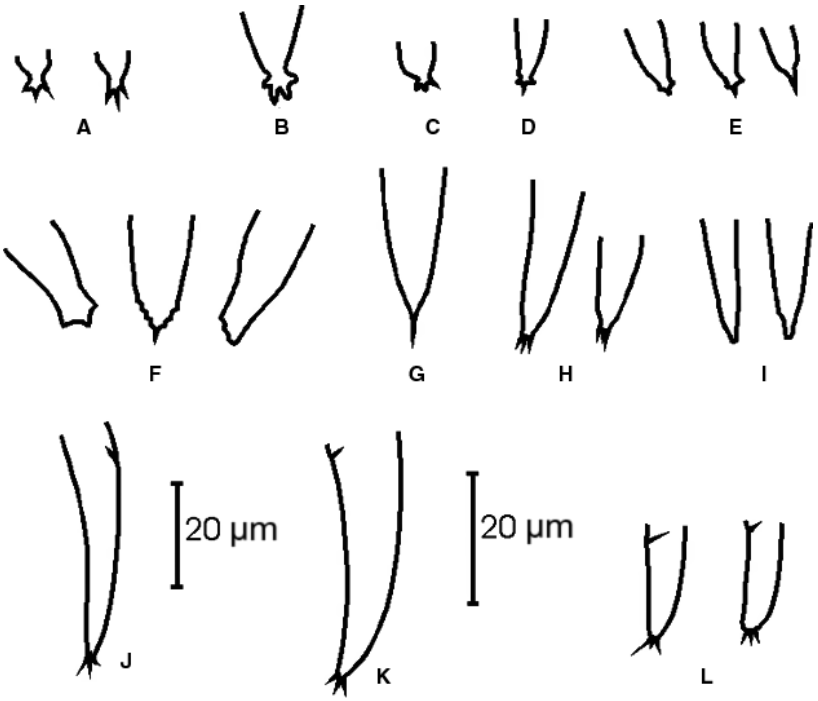

Fig. 10 Supplementary drawings to aid categorization of mucro type and tail shape (scale measurements not provided on many descriptions). 'Star-shape' mucros: (A) *besseyi*, (B) *nonveilleri*, (C) *siddiqii*, (D) *unisexus*, (E) *lichenicola* (described as star-shape, though variants may have an axial ray more prominent than others). 'Leaf-like' mucros: (F) *appendurus* 'single terminal' mucro, (G) *blastophthorus*. 'Box-like' mucros: (H) *ritzemabosi.* No mucro: (I) *fragariae.* Tail shapes: conoid, (J) *besseyi*; elongate-conoid, (K) *aligarhiensis* (described as such by the original description, but could be considered conoid from associated drawing (no '*c*' values available); sub-cylindrical, (L) *siddiqii.*

Table 4. Polytomous key for some of the key characters distinguishing *A. besseyi*

	Code					
Species	A	B	C	D	E	F
A. besseyi	1	1	1	1	1	1
A. hylurgi	1	1	1	1	4	3
A. unisexus	1	1	1/3	1	3	3
A. asteromucronatus	1	1	1/3	2	1	3
A. siddiqii	1	1	3/4	1	1	1/2/3
A. asterocaudatus	1	1/2	1	1	3	3
A. andrassyi	1	1/2	2/3	1/2	2	4
A. wallacei	1	1/2	3	3	1	1
A. goodeyi	1	2	1	1	1	3
A. lichenicola	1	2	1	1/2	1	2/3
A. silvester	1	2	1	1/2	1	4
A. jonesi	1	2	1	1/3	1	2
A. brevistylus	1	2	1/2	2	3	1
A. aligarhiensis	1	2	2/3	1	1	1
A. blastophthorus	2	2	1/2	3	1	2
A. subtenuis	2	2	4	1	2	2/3
A. ritzemabosi	4	2	2	1	1	3
A. fragariae	2/4	2	2	1	3	2/3

Aphelenchoides nonveilleri and *A. saprophilus*, mentioned in previous editions of this key, are now considered to be *species indeterminatae*.

Aphelenchoides besseyi, *A. blastophthorus*, *A. fragariae*, and *A. ritzemabosi*[2] live as parasites in buds and leaves of plants. *Aphelenchoides saprophilus*, a fungivorous species, is also often found in damaged or diseased plant material, including bulbs and corms. Andrássy (2007) provided a key to 47 *Aphelenchoides* species found in Europe, including the six species encountered in buds and leaves. A short dichotomous key to *A. besseyi*, *A. fragariae* and *A. ritzemabosi* is given in Table 5.

4.2. Molecular methods

4.2.1. PCR tests

Two real-time PCR tests are available for the identification of isolated nematodes. The tests are described in Appendix 2 (Rybarczyk-Mydłowska *et al.*, 2012) and Appendix 3 (ClearDetections all-inclusive Real-time PCR kit test based on SSU rDNA).

Chizhov *et al.* (2006) and Khan *et al.* (2012) described options to use sequences from 18S and ITS regions, respectively, to identify *A. besseyi.*

Molecular tests can also be used when morphological identification is uncertain.

As performance characteristics of the different tests vary (in particular regarding their specificity) the choice of test should be made according to the circumstances of use.

4.2.2. DNA barcoding

A protocol for DNA barcoding based on COI, 18S rDNA and 28S rDNA is described in Appendix 3 of PM 7/129 *DNA barcoding as an identification tool for a number of regulated pests: DNA barcoding nematodes* (EPPO, 2016) and can support the identification of *A. besseyi.* Sequences are available in Q-bank (http://www.q-bank.eu/Nematodes/).

5. Reference material

Reference material can be found through different resources (e.g. Q-bank, http://www.q-bank.eu/Nematodes/; NCE, http://www.nce.nu/).

6. Reporting and documentation

Guidelines on reporting and documentation are given in EPPO Standard PM 7/77 *Documentation and reporting on a diagnosis*.

7. Performance criteria

When performance criteria are available, these are provided with the description of the test. Validation data is also available in the EPPO Database on Diagnostic Expertise (http://dc.eppo.int), and consultation of this database is recommended as additional information may be available there (e.g. more detailed information on analytical specificity, full validation reports, etc.).

8. Further information

Further information on this organism can be obtained from:

Table 5. Simplified key to distinguish *A. besseyi, A. fragariae* and *A. ritzemabosi* from other species

1	Post-vulval sac length more than one-third the distance between the vulva and the anus	2
	Post-vulval sac length less than one-third the distance between the vulva and the anus; star-shaped mucro present	*A. besseyi*
2	Lateral field with three or four incisures	3
	Lateral field with two incisures, body slender (a = 45–63), cephalic region almost continuous with body contour	*A. fragariae*
3	Tail terminus with a single mucro	Other species
	Tail terminus with two to four processes pointing posteriorly giving it a paintbrush-like appearance, usually four incisures, stylet about 12 µm long, post-vulval sac usually more than half the distance between the vulva and the anus	*A. ritzemabosi*

[2]The IPPC text refers to *A. subtenuis*; however, this nematode feeds on roots.

Prof. Dr G. Karssen, Plant Protection Service, Ministry of Agriculture, Nature Management and Fisheries, 15 Geertjesweg, PO Box 9102, 6700 HC Wageningen, the Netherlands;

Dr Sue Hockland, Independent Plant Nematology Consultant, Emeritus Fellow of Fera, http://plantparasiticnematodes.com/.

9. Feedback on this diagnostic protocol

If you have any feedback concerning this diagnostic protocol, or any of the tests included, or if you can provide additional validation data for tests included in this protocol that you wish to share please contact diagnostics@eppo.int.

10. Protocol revision

An annual review process is in place to identify the need for revision of diagnostic protocols. Protocols identified as requiring revision are marked as such on the EPPO website.

When errata and corrigenda are in press, this will also be marked on the website.

Acknowledgements

This Protocol was originally drafted by S. Hockland (formerly) Food and Environmantal Research Agency, York (GB), revised by V. Gaar, Central Institute for Supervising and Testing in Agriculture, Prague (CZ) with support from S. Hockland, G. Anthoine (ANSES, FR), Renske Landeweert (ClearDetections, NL) and M. Mota (University of Evora, PT). It was reviewed by the Panel on Diagnostics in Nematology.

References

Allen MW (1952) Taxonomic status of the bud and leaf nematodes related to *Aphelenchoides fragariae* (Ritzema Bos, 1891). *Proceedings of the Helminthological Society of Washington* **19**, 108–120.

Andrássy I (2007) Free-living nematodes of Hungary (*Nematoda errantia*), Vol. II. In: *Pedozoologica Hungarica No. 4* (Ed. Csuzdi C & Mahunka S), pp. 18–22. Hungarian Natural History Museum and Systematic Zoology Research Group of the Hungarian Academy of Sciences, Budapest (HU). 496 pp.

Baranovskaya IA (1981) [Nematodes of Soil and Plants (aphelenchoidids and seinurids).]. Moscow, Nauka. 233 pp (in Russian).

CABI (2013) *Aphelenchoides besseyi*. Crop Protection Compendium 2013. CABI, Wallingford (UK).

Chaves N, Cervantes E, Zabalgogeazcoa I & Araya C (2013) *Aphelenchoides besseyi* Christie (Nematoda: Aphelenchoididae), agente causal del amachamiento del frijol común. *Tropical Plant Pathology* **38**, 243–252.

Chizhov VN, Chumakova OA, Subbotin SA & Baldwin JG (2006) Morphological and molecular characterization of foliar nematodes of the genus *Aphelenchoides*: *A. fragariae* and *A. ritzemabosi* (Nematoda: Aphelenchoididae) from the Main Botanical Garden of the Russian Academy of Sciences, Moscow. *Russian Journal of Nematology* **14**, 179–184.

Dastur JF (1936) A nematode disease of rice in the Central Provinces. *Proceedings of the Indian Academy of Sciences, Section B* **4**, 108–121.

Deimi AM, Maafi ZT, Rius JEP & Castillo P (2006) *Aphelenchoides subtenuis* (Cobb, 1926) Steiner & Buhrer, 1932 (Nematoda: Aphelenchoididae) from Iran with morphological and morphometric characterization. *Nematology* **8**, 903–908.

EPPO (2004) PM 7/39(1) *Aphelenchoides besseyi*. *EPPO Bulletin* **34**, 303–308.

EPPO (2013) PM 7/119 (1) Nematode extraction. *Bulletin OEPP/EPPO Bulletin* **43**, 471–495.

EPPO (2016) PM 7/129 DNA barcoding as an identification tool for a number of regulated pests. *EPPO Bulletin* **46**, 501–537.

Fortuner R (1970) On the morphology of *Aphelenchoides besseyi* Christie, 1942 and *A. siddiqii* n.sp. *Journal of Helminthology* **44**, 141–152.

Franklin MT & Siddiqi MR (1972) *Aphelenchoides besseyi. CIH Descriptions of Plant-Parasitic Nematodes*. Set 1, no. 4. CAB International, Wallingford (GB).

Hockland S (2002) A pragmatic approach to identifying *Aphelenchoides* species for plant health quarantine and pest management programmes. PhD Thesis, University of Reading (GB).

Hockland S & Eng L (1997) *Capsicum annuum v. longum*: A new host record for the rice white tip nematode, *Aphelenchoides besseyi*. *International Journal of Nematology* **7**, 229.

Holterman M, van der Wurff A, van den Elsen S, van Megen H, Bongers T, Holovachov O *et al.* (2006) Phylum-wide analysis of SSU rDNA reveals deep phylogenetic relationships among nematodes and accelerated evolution toward crown clades. *Molecular Biology and Evolution* **23**, 1792–1800.

Hoshino S & Togashi K (1999) A simple method for determining *Aphelenchoides besseyi* infestation level of *Oryza sativa* seeds. *Journal of Nematology* **31**(Suppl.), 641–643.

Hunt DJ (1993) *Aphelenchoides besseyi*. Species description. In: *Aphelenchida, Longidoridae and Trichodoridae, their Systematics and Bionomics*, pp. 56–58. CAB International, Wallingford (GB).

Ibrahim SK, Perry RN, Burrows PR & Hooper DJ (1994a) Differentiation of species and populations of *Aphelenchoides* and of *Ditylenchus augustus* using a fragment of ribosomal DNA. *Journal of Nematology* **26**, 41–421.

Ibrahim SK, Perry RN & Hooper DJ (1994b) Use of esterase and protein patterns to differentiate two new species of *Aphelenchoides* on rice from other species of *Aphelenchoides* and from *Ditylenchus augustus* and *D. myceliophagus*. *Journal of Nematology* **40**, 267–275.

IPPC (2016) *Annex to ISPM 27 – Aphelenchoides besseyi, A. fragariae and A. ritzemabosi (2006-025)*. https://www.ippc.int/en/publications/83447/ [accessed on 01 Sep 2016]

ISTA (2017) 7-025 Detection of *Aphelenchoides besseyi* on *Oryza sativa*. Version 1.13, p. 7-025-1, 7-025-5.

Khan MR, Handoo ZA, Rao U, Rao SB & Prasad JS (2012) Observations on the foliar nematode, *Aphelenchoides besseyi,* infecting tuberose and rice in India. *Journal of Nematology* **44**, 391–398.

Liu W, Lin M, Li H & Sun M (2008) Dynamic development of *Aphelenchoides besseyi* on rice plant by artificial inoculation in the greenhouse. *Agricultural Sciences in China* **7**, 970–976.

Moretti F, Cotroneo A, Tacconi R, Santi R & De Vincentis F (1999) Damage from *Aphelenchoides besseyi* on rice and nematode extraction methods from rice seeds. *Informatore Fitopatologico* **3**, 39–41, (in Italian).

Perry RN & Moens M (2006) *Plant nematology*, pp. 568, CABI Publishing, Wallingford (GB).

Rybarczyk-Mydłowska K, Mooyman P, van Megen H, van den Elsen S, Vervoort M, Veenhuizen P *et al.* (2012) Small subunit ribosomal

DNA-based phylogenetic analysis of foliar nematodes (*Aphelenchoides* spp.) and their quantitative detection in complex DNA backgrounds. *Phytopathology* **102**, 1153–1160.

Sánchez-Monge A, Flores L, Salazar L, Hockland S & Bert W (2015) An updated list of the plants associated with plant-parasitic *Aphelenchoides* (Nematoda: Aphelenchoididae) and its implications for plant-parasitism within this genus. *Zootaxa* **4013**, 207–224.

Sanwal KC (1961) A key to species of the nematode genus *Aphelenchoides* Fischer, 1894. *Canadian Journal of Zoology* **39**, 143–148.

Shahina F (1996) A diagnostic compendium of the genus *Aphelenchoides* Fischer, 1894 (Nematoda: Aphelenchida) with some new records of the group from Pakistan. *Pakistan Journal of Nematology* **14**, 1–32.

Tamura I & Kegasawa K (1957–1959) Studies on the ecology of the rice nematode, Aphelenchoides besseyi Christie. I. On the swimming away of rice nematodes from the seeds soaked in water and its relation to the water temperature. II. On the parasitic ability of rice nematode and their movement into hills. III. The injured features of the rice plant and the population density of nematodes found in the unhulled rice grain with special reference to the type of nursery bed. IV. The injurious features and population dynamics of nematodes in unhulled rice grain with special reference to the cultural environment of rice plant. *Japanese Journal of Ecology* **7**:111–114, 1957, 8:37-42, 1958, 9:1-4, 65-68, 1959. (Japanese, English Summaries).

Todd EH & Atkins JG (1958) White tip disease of rice. I. Symptoms, laboratory culture of nematodes, and pathogenicity tests. *Phytopathology* **48**, 632–637.

Uebayashi Y, Amano T & Nakanishi I (1976) Studies on the abnormal rice kernel "Kokutenmai". V. Mechanism of the symptoms development. *Japanese Journal of Nematology* **6**, 67–72.

Wang X, Wang P, Gu JF, Wang JL & Li HM (2013) Description of *Aphelenchoides xui* sp. n. (Nematoda: Aphelenchoididae) in packaging wood from South Africa. *Nematology* **15**, 279–289.

Yoshii H & Yamamoto S (1950) A rice nematode disease "Senchû Shingare Byô" symptom and pathogenic nematode. *Journal of the Faculty of Agriculture* **9**, 209–222.

Yoshii H & Yamamoto S (1951) [On some methods for the control of the rice nematode disease.]. *Science Bulletin of the Faculty of Agriculture, Kyushu University* **12**, 123–131 (in Japanese).

Yu PC & Tsay TT (2003) Occurrence of a foliar nematode disease of fern in Taiwan. *Plant Pathology Bulletin* **13**, 35–44.

Appendix 1 – Extraction from seeds

A. Extraction method by the ISTA

Sample and subsample size

The sample (total number of seeds tested) and subsample size to be tested depends on the desired tolerance standard (maximum acceptable percentage of seeds infested) and detection limit (theoretical minimum number of pathogen propagules per seed which can be detected).

Materials

Mill: e.g. Husker TR-120 (Kett Electric Laboratory, Japan)

Containers: beakers 45 mm diameter

Counting dish: any standard nematode counting dish (e.g. 90 mm diameter De Grisse dish)

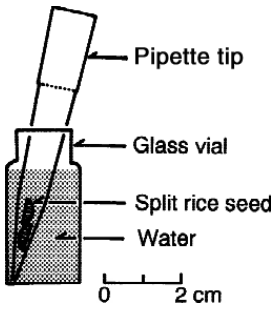

Fig. 11 Illustration of the extraction method from Hoshino & Togashi.

Sieves: nylon, with mesh of 0.25 mm

Incubator: operating at 25 ± 2°C

Microscope: dissecting microscope, magnification ×50; high-power microscope, magnification ×1000

Method

Dehull the seeds using a mill with a distance of 1 mm between the rolls (CCP).

Fit a nylon sieve, with a mesh of 0.25 mm, into a beaker of 45 mm diameter and transfer kernels and hulls onto the nylon sieve. Fill this beaker with 20 mL of water.

Leave the beaker undisturbed for 24 h at 25 ± 2°C.

Remove the sieve from the beaker and squeeze gently.

B. Extraction method from Hoshino & Togashi

Rice seeds are cut longitudinally in two with small pruning scissors, then transferred into single plastic pipette (Fig. 11).

Tips containing a split seed are then placed singly upright in glass vials (6.5 mL capacity) with water. Nematode extraction with both procedures is conducted in the dark at approximately 25°C (Tamura and Kegasawa, 1957).

Appendix 2 – Identification by real-time PCR with specific primers (Rybarczyk-Mydłowska *et al.*, 2012)

1. General information

Scope of the test: identification of single *A. besseyi* nematodes by real-time PCR and detection of *A. besseyi* nematodes in both simple (plant material) and complex (soil or substrate) DNA backgrounds by real-time PCR.

1.1 This test was described in Rybarczyk-Mydłowska *et al.* (2012).

1.2 This test targets the SSU rDNA gene.

1.3 The amplicon is 325 base pairs long.

1.4 Oligonucleotides: Forward primer: 1770–5′gcg gga ttc gtg gtt c*t-3′) (*locked nucleic acids). Reverse primer: 1772–5′cga cat gcc gaa aca tga g-3′.

1.5 This test was developed on an iQ5 real-time PCR system (Bio-Rad, Hercules, CA).

2. Methods

2.1 Nucleic acid extraction

2.1.1 DNA is extracted from single nematodes and from nematode suspensions.

2.1.2 DNA is extracted according to Holterman *et al.* (2006). Single nematodes are transferred to a 0.2 mL PCR tube containing 25 µL of sterile water. An equal volume of lysis buffer containing 0.2 M NaCl, 0.2 M Tris–HCl (pH 8.0), 1% (v/v) β-mercaptoethanol and 800 µg/mL proteinase-K was added. Lysis took place in a thermomixer (Eppendorf, Hamburg, Germany) at 65°C and 750 rpm for 2 h, followed by incubation for 5 min at 100°C. Lysate was used immediately or stored at −20°C.

2.2 Real-time PCR

2.2.1 Master mix

Reagent	Working concentration	Volume per reaction (µL)	Final concentration
Molecular-grade water*	N.A.	8.5	N.A.
Real-time PCR buffer (Absolute SYBR Green fluorescein mix, Thermo Fisher, Wilmington, DE)	2×	12.5	1×
Forward primer 1770	10 µM	0.5	0.2 µM
Reverse primer 1772	10 µM	0.5	0.2 µM
Subtotal		22	
DNA solution		3	
Total		25	

*Molecular-grade water should be used preferably. Alternatively, sterile (autoclaved or 0.45 µm filtered), purified (deionized or distilled) and nuclease-free water can be used.

2.2.2 PCR cycling conditions: Initial denaturation 95°C for 15 min; followed by 60 cycles of 95°C for 30 s, 63°C for 1 min, and 72°C for 30 s.

3. Essential procedural information

3.1 Controls

For a reliable test result to be obtained, the following controls should be included for each series of nucleic acid extraction and amplification of the target organism and target nucleic acid, respectively:

Negative isolation control (NIC) to monitor contamination during nucleic acid extraction: nucleic acid extraction and subsequent amplification preferably clean extraction buffer.

Negative amplification control (NAC) to rule out false positives due to contamination during the preparation of the reaction mix: amplification of molecular-grade water that was used to prepare the reaction mix.

Positive amplification control (PAC) to monitor the efficiency of the amplification: amplification of nucleic acid of the target organism. This can include nucleic acid extracted from the target organism, or a synthetic control (e.g. a cloned PCR product).

3.2 Interpretation of results: in order to assign results from PCR-based test the following criteria should be followed:

Verification of the controls

- The PAC amplification curves should be exponential
- NIC and NAC should give no amplification.

When these conditions are met:

- A test will be considered positive if it produces an exponential amplification curve
- A test will be considered negative if it does not produce an exponential amplification curve
- Additionally for this SYBR® Green based real-time PCR test, the melting temperature (T_M) value should be as expected
- Tests should be repeated if any contradictory or unclear results are obtained.

4. Performance criteria available

Minimum requirements should be made in line with PM 7/98.

4.1 Analytical sensitivity data: not available

4.2 Analytical specificity data: this test was evaluated against 11 non-target organisms that were defined as the closest non-target organisms identified *in silico* (after the changing mismatch setting of the primer design software used, ARB). To test the specificity of the primers, bacterial clones harbouring a SSU rDNA fragment were used as the DNA source under artificial conditions: *Acrobeloides* cf. *thornei* 1 (JQ957903), *Ascolaimus* cf. *elongates* 2 (EF591330), *Aphelenchoides ritzemabosi* 2, *Clavicaudoides trophurus* 1 (AY284772), *Deladenus durus* 1 (JQ957898), *Domorganus macronephritices* 2 (FJ969122), *Ethmolaimus pratensis* 1 (AY593942), *Panagrobelus stammeri* 1 (AF202153), *Paracyatholaimus intermedius* 3 (JQ957906), *Rotylenchus uniformis* (AY593882), *Tripyla cf filicaudata* 1 (AY284730)

4.3 Data on repeatability: not available

4.4 Data on reproducibility: not available

Appendix 3 – Diagnostic real-time PCR test for identification and detection of *A. besseyi*, based on SSU rDNA

1. General Information

1.1 Scope of the test: identification of single *A. besseyi* nematodes by real-time PCR and detection of

A. besseyi nematodes in both simple (plant material) and complex (soil or substrate) DNA backgrounds by real-time PCR.

1.2 This test is available as an all-inclusive real-time PCR kit (ClearDetections, the Netherlands; http://www.clearDetections.com)

1.3 This test targets the SSU rDNA gene.

1.4 The amplicon is over 300 base pairs long.

1.5 Oligonucleotide sequences are not disclosed.

1.6 This test was developed on an iQ5 Real-time PCR system (Bio-Rad, Hercules, CA).

2. Methods

2.1 Nucleic acid extraction

This real-time PCR test can be combined with any nematode DNA extraction method delivering target DNA. When using this test for nematode quantification purposes it is highly recommended to include an (internal or external) DNA standard in the extraction procedure to correct for potential DNA losses during the DNA extraction and purification process. The all-inclusive kit contains a separate real-time PCR primer set for the detection of 'nematode DNA', which can be used when in doubt about the presence of nematode DNA in a DNA sample.

2.2 Real-time PCR

All necessary real-time PCR test components are included in the real-time PCR kit:

Real-time PCR primer set (species-specific, forward and reverse)

- Positive amplification control (PAC)
- DNA dilution buffer (DNase/RNase free)
- PCR enhancer (for optimal PCR performance)
- PCR mix with fluorescent DNA-binding dye
- General nematode DNA real-time PCR primer set (for troubleshooting purposes)
- Bench-side protocol.

2.2.1 PCR cycling conditions: 3 min 95°C, 35 cycles of 10 s 95°C, 1 min 63°C, 30 s 72°C, 0.2–0.5°C steps 72°C→95°C

3. Essential procedural information

3.1 Controls

For a reliable test result to be obtained, the following controls should be included for each series of nucleic acid extraction and amplification of the target organism and target nucleic acid, respectively:

Negative isolation control (NIC) to monitor contamination during nucleic acid extraction: nucleic acid extraction and subsequent amplification preferably clean extraction buffer.

Negative amplification control (NAC) to rule out false positives due to contamination during the preparation of the reaction mix: amplification of molecular-grade water that was used to prepare the reaction mix.

Positive amplification control (PAC, included in the kit) to monitor the efficiency of the amplification: amplification of nucleic acid of the target organism. This can include nucleic acid extracted from the target organism or a synthetic control (e.g. a cloned PCR product).

3.2 Interpretation of results: in order to assign results from PCR-based tests the following criteria should be followed:

Verification of the controls:

- The PAC amplification curves should be exponential
- NIC and NAC should give no amplification.

When these conditions are met:

- A test will be considered positive if it produces an exponential amplification curve
- A test will be considered negative if it does not produce an exponential amplification curve
- A melt curve analyses is performed and the obtained T_M value equals the T_M value of the PAC
- Tests should be repeated if any contradictory or unclear results are obtained
- The real-time PCR primer set included in the kit for the detection of 'nematode DNA' can be used when in doubt about the presence of nematode DNA in a DNA sample (check for possible false negatives).

4. Performance criteria available

This real-time PCR test is validated in line with PM 7/98.

4.1 Analytical sensitivity: less than one individual nematode

4.2 Diagnostic sensitivity: 100%

4.3 Analytical specificitySpecificity value 100%

Number of strains/populations of target organisms tested: *A. besseyi* (populations 2160 and E9192) obtained from the Dutch NPPO (ref. Prof. Gerrit Karssen)

Number of non-target organisms tested: nematode suspensions obtained from plant material; single *A. subtenuis*; single *A. fragariae*; single *A. ritzemabosi*; single *A. saprophilus*; single *Ditylenchus dipsaci*; single *Ditylenchus destructor.*

4.4 Diagnostic specificity: 100%

4.5 Reproducibility: 100%

4.6 Repeatability: 100%

4.7 Accuracy: 100%

4.8 Dynamic range: between 10–100 and 0.1 billion copies of target DNA

4.9 Selectivity: 100%

4.10 Robustness: OK

Appendix 4 – Database of morphological characters for *A. besseyi* and selected species

Species	Mucro shape	Length of post-vulval sac (pvs)	Tail shape	Position of excretory pore (ep) and nerve ring (nr)	*a*	*b*	Length (mm)	Stylet	L.L.	*c*
A. aligarhiensis	Star	×5.5 body width, extending to more than 50% of v–a distance	Elongate-conoid	ep slightly anterior to nr	25–35	7.0–9.0	0.50–0.70	10	4	13–22
A. andrassyi	Star	×3 vulval body width	Elongate-conoid	Not possible to advise	23–28	3.2–3.9	0.39–0.44	9.0–10.0	3	6.0–12.0
A. asterocaudatus	Star	×2 vulval body width	Conoid	ep posterior to nr	24.6	9.6	0.62	12	2	16
A. asteromucronatus	Star	×1 vulval body width or less	Conoid	ep at level of lower edge of nr	32–39	5.5–9.5	0.39–0.54	9	4	10.9–14.5
A. besseyi first description	Star	2.5–3.5 anal body width but less than	Conoid	ep usually near the anterior edge of nr	32–42	10.2–11.4	0.66–0.75	10–12.5	4	17–21
(all descriptions)	(star)	33% v–a distance	Conoid	(ditto)	26.6–58	9.0–13.1	0.57–0.88	10–12.5	4	13.8–21
A. blastophthorus	Single terminal mucro	Approx. 50% v–a distance	Conoid	ep approx. opposite nr	32–47	9.3–11	0.68–0.9	15–19.5	4	16–21
A. brevistylus	Star	33–66% v–a distance	Conoid	ep anterior to nr	29.1 –35.0	8.1–10.5	0.39–0.63	6.0–8.0	2	11.1–15.7
*A. fragariae**	No mucro (sometimes a blunt spike presents)	More than 50% v–a distance	Elongate-conoid	ep level with or close behind nr	45–63	8–15	0.45–0.80	10–11	2	12–20
A. goodeyi	Star	×3 vulval body width	Convex-conoid	ep close behind nr, level with its hind edge	29–39	n/a	0.46–0.61	11.5–12.5	4	14–18
A. hylurgi	Star	×1.5 body width	Conoid	ep slightly posterior to nr	26.6	10.2	0.57	13	Obscure	14.7
A. jonesi	Star	Nearly ×2 body widths long. nearly 50% v–a distance	Conoid	ep opposite nr	20–28	9.3–11.0	0.72–0.99	11.0–14.0	4	16–22
A. lichenicola	Star	50% or more v–a distance	Elongate-conoid	ep opposite or close to posterior margins of nr	32–43	7.0–10.5	0.53–0.69	9.5–10	4	15–17
A. nonveilleri	Star	×3 body width	Conoid	Not known	31	n/a	0.59	12.8	3	17
A. ritzemabosi	Tail terminus invariably ending in a box-like structure which has two to four minute processes pointing posteriorly	50% or more the v–a distance	Elongate-conoid	ep 0.5–2 body widths posterior to nr	40–45	10–13	0.77–1.20	12	4	18–24

(continued)

Table *(continued)*

Species	Mucro shape	Length of post-vulval sac (pvs)	Tail shape	Position of excretory pore (ep) and nerve ring (nr)	*a*	*b*	Length (mm)	Stylet	L.L.	*c*
A. siddiqii	Star	×0.5–1.0 body width	Subcylindrical	ep usually opposite the posterior margins of nr, sometimes reaching near its anterior margins	26.7–38.9	7.1–9.7	0.37–0.70	11–12.5	4	14.1–19.6
A. silvester	Star	No information	Convex-conoid	No information	37–38	8.0–9.7	0.48–0.56	9.5–10	4	15–16
A. subtenuis[*]	Single ventral mucro	58–80% v–a distance	Cylindroid	ep at level of, or posterior to, nerve ring	45–68	12–17	0.69–1.10	11–13	3	22–28
A. unisexus	Star	20–33% v–a distance	Conoid	ep at level of posterior margin of nr, or just posterior to it	30–36.9	7.9 –10.2	0.48–0.76	10.0–11.0	2	13.0–17.5
A. wallacei	Star	×2 body widths long	Convex-conoid	ep anterior to nr	22–23	7.8–8.5	0.69–0.73	13.5–14	4	15–17

[*]Data from more than one source.